JOINT INSTITUTE FOR NUCLEAR RESEARCH
Flerov Laboratory of Nuclear Reactions

FINAL REPORT ON THE INTEREST PROGRAMME

Optimization of the solid ISOL method for volatile reaction products of heavy ion beam reactions

Supervisor:
Dr. Vedeneev Viacheslav Yurievich

Student:
Md Majid Hussain, India
Indian Institute of Engineering Science and Technology, Shibpur.

Participation period:
October 20 – November 30, Wave 13
Dubna, 2025

Abstract

This project analyzes the performance of the solid-state ISOL system at the MASHA mass separator for optimal separation and detection of volatile reaction products from heavy-ion reactions ^{40}Ar + ^{166}Er, ^{40}Ar + ^{148}Sm, and ^{48}Ca + ^{242}Pu, producing neutron-deficient Hg and Rn isotopes. Using Origin Pro, alpha-decay spectra were processed through stepwise plotting, peak fitting, and channel-to-energy calibration to reconstruct decay chains and generate energy-position heat maps, enabling clear visualization of isotope distributions over detector strips without performing new experiments. The study benchmarks the upgraded MASHA setup, including rotating target box with hot catcher, ECR ion source, and optimized transport conditions, which together enhance ISOL-based mass identification and decay studies of short-lived superheavy nuclei. These results support ongoing searches near the predicted island of stability and provide practical guidance for further optimization of solid catcher materials and high-temperature ISOL operation for SHE experiments at FLNR JINR.

1. Introduction

The production and study of superheavy elements (SHE) are strongly connected to the evolution of heavy-ion accelerators, starting from the early cyclotrons at JINR Dubna, which provided intense beams for fusion reactions and opened access to ever-heavier nuclei. Modern SHE research combines such accelerators with advanced separators to extend the periodic table and probe exotic nuclei where shell effects dominate and production cross sections are extremely small. In this context, the MASHA (Mass Analyzer of Super Heavy Atoms) facility at the Flerov Laboratory of Nuclear Reactions (FLNR) is designed to determine mass-to-charge ratios of heavy reaction products while simultaneously detecting their α decays and spontaneous fission, which are crucial observables for reliable nuclide identification MASHA operates using a solid-state ISOL (Isotope Separation On-Line) scheme: fusion-evaporation residues are stopped in a high-temperature catcher, volatile species are released, ionized, mass-separated, and finally implanted into position-sensitive silicon detectors for decay spectroscopy. This approach is particularly effective for volatile elements such as radon and mercury. In my project, fusion reactions ^{40}Ar + ^{166}Er, ^{40}Ar + ^{148}Sm, and ^{48}Ca + ^{242}Pu were used to produce neutron-deficient Hg and Rn isotopes, and MASHA data were analyzed to construct one-dimensional α-energy spectra and two-dimensional energy–position maps, followed by energy calibration using known reference α lines and comparison with evaluated decay schemes to assign isotope identities. The broader motivation is to optimize the solid ISOL technique and MASHA's separation efficiency for volatile reaction products, thereby enhancing sensitivity and selectivity in future SHE searches and contributing to precision studies of nuclei near key neutron shell closures and the predicted "island of stability".

2. MASHA Setup

The upgrade of some parts of MASHA setup was done during the last years. First of all, target box, ion source, data acquisition system, beam diagnostics and control system were modified.

A schematic overview of the system target + catcher is shown in Fig. 1a. This uses the block of rotating targets, assembled into cassettes, which is presented at Fig. 1b. The idea to use rotating target instead stationary is better efficiency and heat distribution. A photo of a target disc with 242Pu as a target is shown in Fig. 1b. The disc rotated at the frequency of 25 Hz via Siemens electric engine. Changings touched a heater also. Now it's fully modified and represents thermally expanded graphite heated directly by current. This removes the heating losses and irregularity of the heating. The division foil was changed to thin graphite foil in connection to its thermal reliability in comparison to titanium foil.

2.1 Ion Source

The ion source is operated under ultra-high frequency conditions at about 2.45 GHz. The incoming atoms of nuclear reaction products are ionized to the charge state Q = +1 and accelerated up to 38 keV by a three-electrode electrostatic lens. The ion beam formed is separated by the magneto-optical mass-to-charge ratio analyzer after. Obtained for noble gases, the ionization efficiency is about 90 % . Traditionally the noble gases (krypton**,** xenon) are chosen for the optimization of the ECR ion source parameters because of its first ionization potentials have maximum values (VIII group of the periodic table) and these are chemical inert elements. For other elements it could differ much, but in the present article it will be compared with Hg, which is proposed to be chemical analogue of Copernicium, with inert gas.

Life time of atoms on the walls depends on the chemical inertia of the wall surface. The walls of the source chamber are covered by titanium nitride (TiN which is chemical inert compound) as well as the walls of catcher and transportation line between. This is made because mercury has a large adhesion on steel and when the atom goes inside the chamber it makes multiple collisions with walls before it ionizes. So, it means that the neutral atom have a very large possibility to "sit" at walls and not to be ionized. That is why a suggestion to cover stainless steel with TiN, which is chemically close to ceramic, was made. Therefore, the ionization efficiency and outgoing time crucially increased. For other elements, such as inert gases the covering affects does not affect or have a minor affect to increase efficiency. The effective using of ion source is to get the most suitable parameters for power, frequency of microwave generator and the pressure of the buffer gas. Helium is injected in small proportions through piezoelectric valve to reach the pressure at about $10-5$ mbar, microwave radiation at frequency 2.45 GHz and power from 20 to 60 Watts to gather the stable plasma inside. At these conditions we get beam current ~600–700 μA of the helium mixture in case if the whole wave is absorbed by the source.

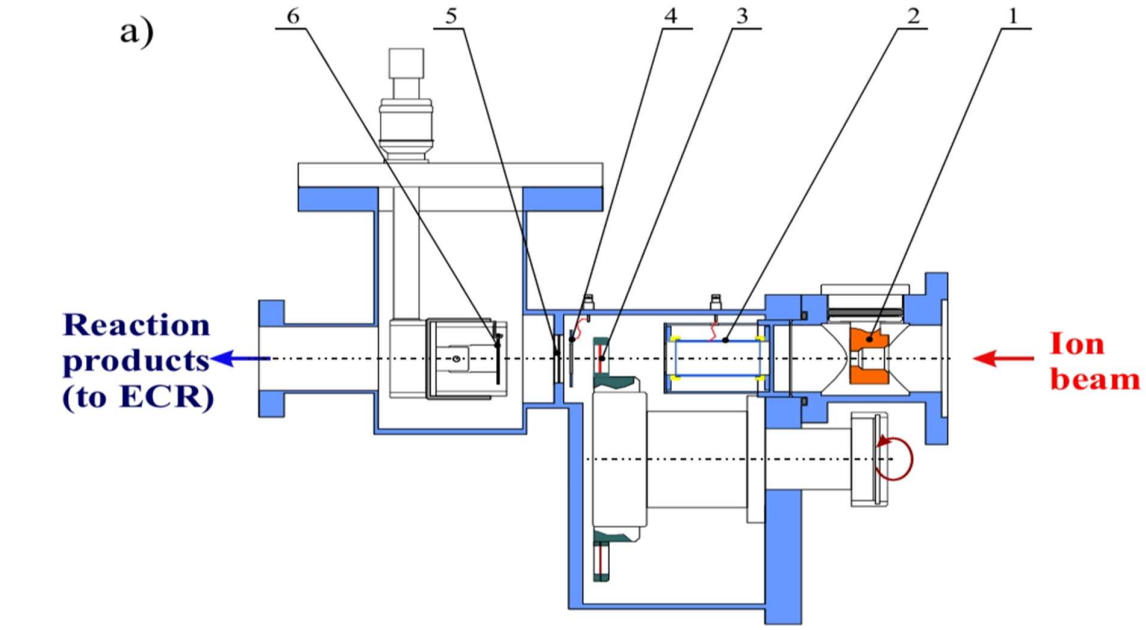

Fig. 1 (a) Schematic overview of the target-hot catcher system. Here: 1– diaphragm; 2– pick-up sensor; 3 target on the wheel; 4– electron emission beam monitor; 5– separating foil; 6– hot catcher. **1(b)** The photo of the rotating target cassette in assembly. 6 packs, 2 windows at 14 mm width each. Target material– 242Pu in oxide state put on the Ti 2 μm thick foil.

3. EXPERIMENTAL DATA ANALYSIS AND DATA PROCESSIONG

In nuclear spectroscopy, alpha-decay spectra are crucial for understanding the structure and stability of heavy nuclei. Here, we analyzed three complete-fusion reactions:

I. **^{40}Ar + ^{148}Sm** producing isotopes ^{180}Hg to ^{185}Hg.
II. **^{40}Ar + ^{166}Er** producing isotopes ^{201}Rn to ^{205}Rn.
III. **^{48}Ca + ^{242}Pu** producing isotopes ^{212}Rn, ^{218}Rn, and ^{219}Rn

3.1 Basic Reaction Scheme for ^{40}Ar + ^{148}Sm

Fusion forms the compound nucleus,

Where ^{188}Hg* is an excited compound nucleus. De-excitation proceeds through an emission of a few neutrons, giving evaporation residues

$$^{188}\mathrm{Hg}^{*} \rightarrow {}^{(188-xn)}\mathrm{Hg} + xn$$

Experiments with the ^{40}Ar + ^{148}Sm system report production of the following Hg isotopes as main residues: ^{180}Hg,^{181}Hg,^{182}Hg,^{183}Hg,^{184}Hg,^{185}Hg.

3.2 Basic Reaction Scheme for ^{40}Ar + ^{166}Er

The reaction ^{40}Ar + ^{166}Er forms a compound nucleus ^{206}Rn*, which then evaporates neutrons to produce the isotopes ^{201}Rn to ^{205}Rn.

$$^{40}\mathrm{Ar} + {}^{166}\mathrm{Er} \rightarrow {}^{206}\mathrm{Rn}^{*}$$

Forming an excited compound nucleus with mass 206 and $Z = 86$ (Rn).

Neutron evaporation channels:

$$^{206}\mathrm{Rn}^{*} \rightarrow {}^{(206-xn)}\mathrm{Rn} + xn \quad x=1–5$$

3.3 Basic Reaction Scheme for ^{48}Ca + ^{242}Pu

The multinucleon transfer reaction has been used at MASHA (FLNR JINR) to produce and study the radon isotopes

$$^{48}\mathrm{Ca} + {}^{242}\mathrm{Pu} \rightarrow {}^{212,218,219}\mathrm{Rn} + \text{(other fragments, n, p, α…)}$$

4. Histograms for Hg ($^{40}Ar + ^{148}Sm$)

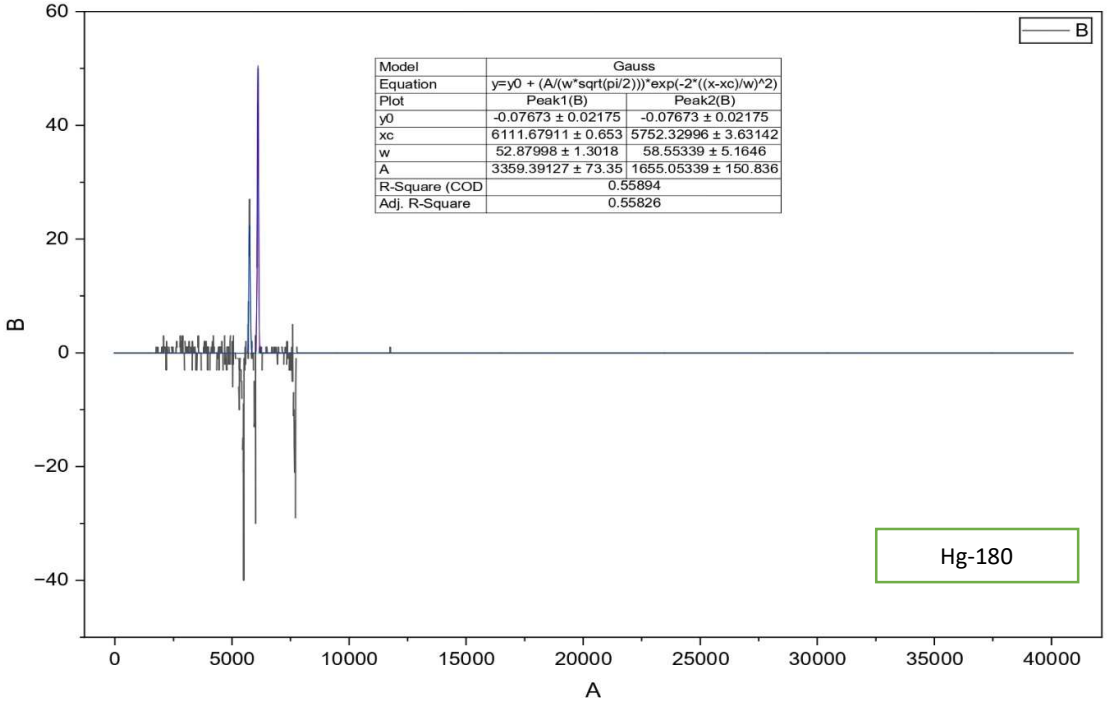

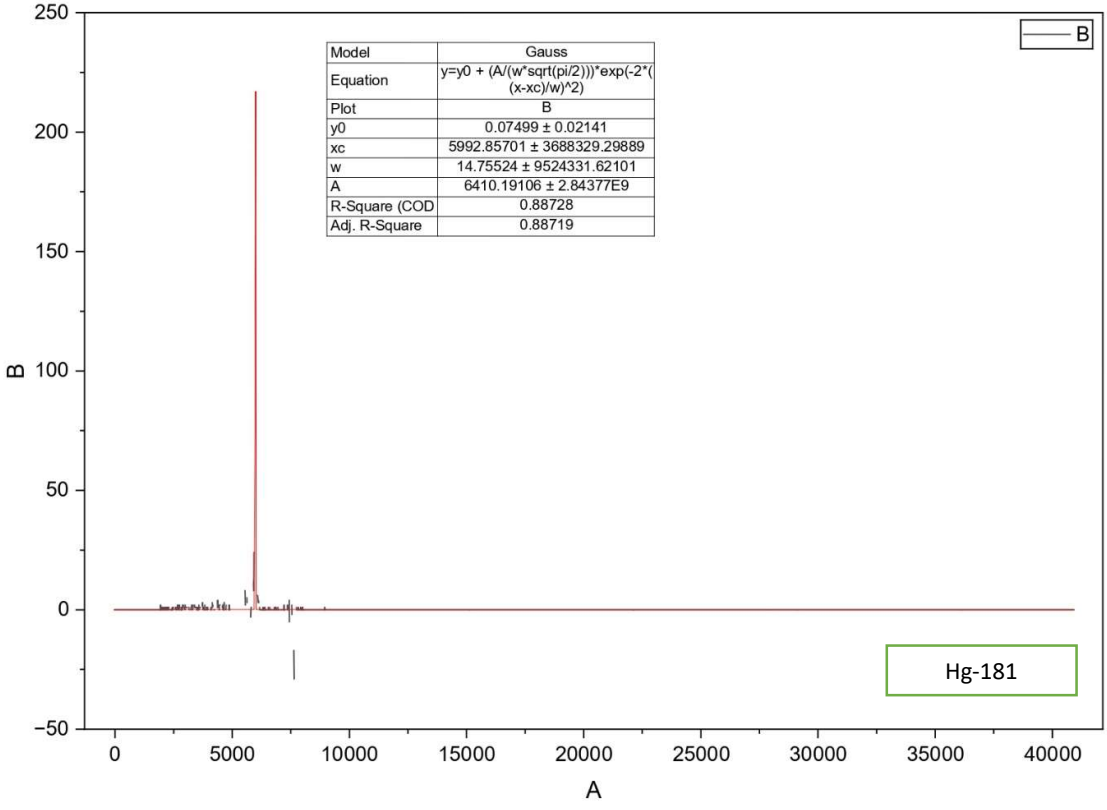

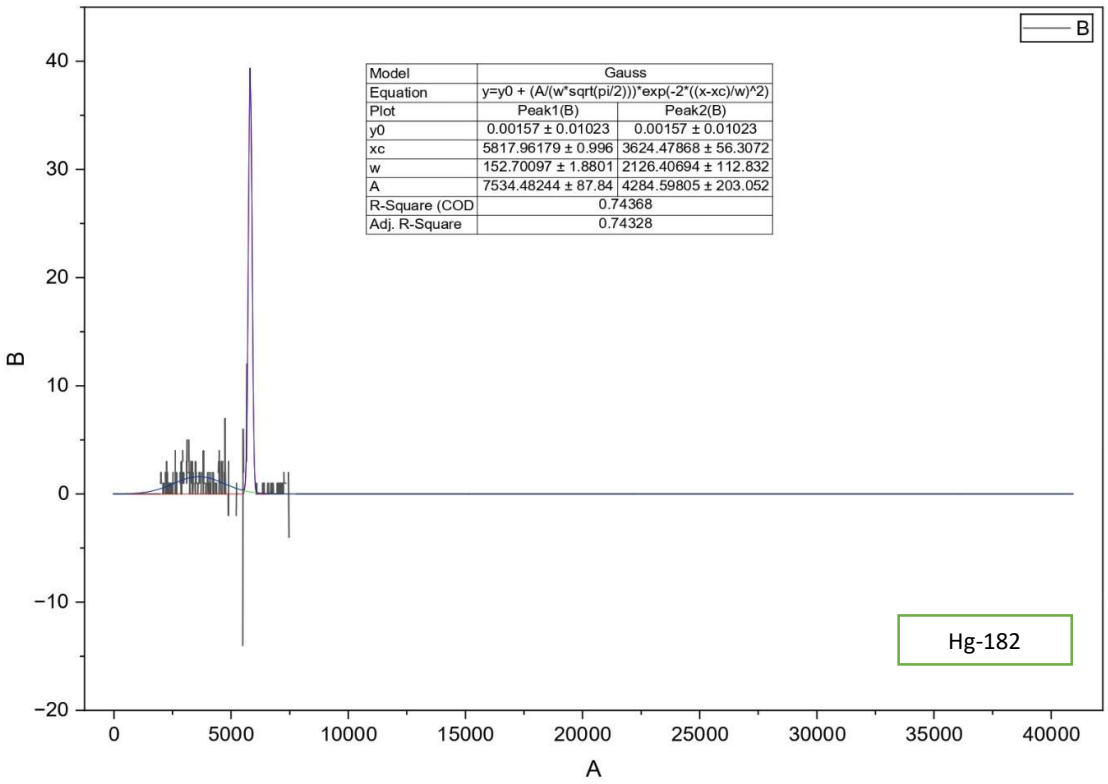
B
Model Gauss
Equation y=y0 + (A/(w*sqrt(pi/2)))*exp(-2*((x-xc)/w)^2)
Plot Peak1(B) Peak2(B)
y0 0.00157 ± 0.01023 0.00157 ± 0.01023
xc 5817.96179 ± 0.996 3624.47868 ± 56.3072
w 152.70097 ± 1.8801 2126.40694 ± 112.832
A 7534.48244 ± 87.84 4284.59805 ± 203.052
R-Square (COD 0.74368
Adj. R-Square 0.74328
Hg-182
B
A

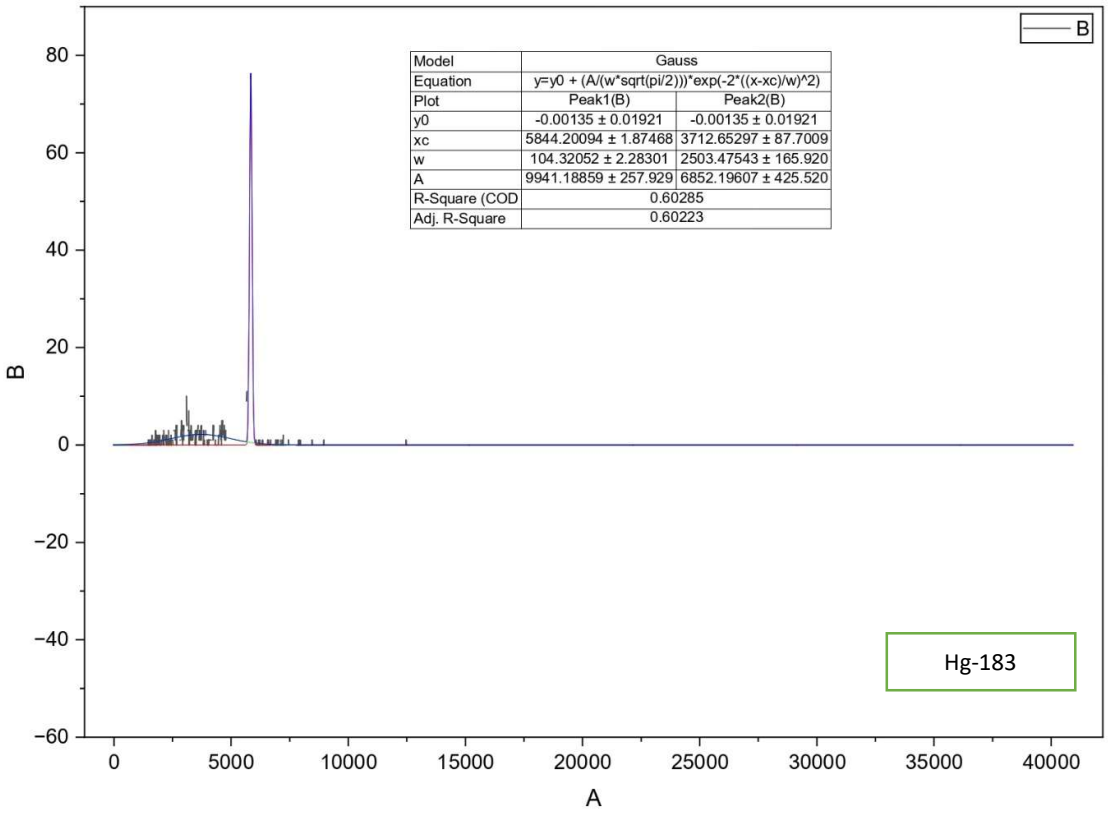
B
Model Gauss
Equation y=y0 + (A/(w*sqrt(pi/2)))*exp(-2*((x-xc)/w)^2)
Plot Peak1(B) Peak2(B)
y0 -0.00135 ± 0.01921 -0.00135 ± 0.01921
xc 5844.20094 ± 1.87468 3712.65297 ± 87.7009
w 104.32052 ± 2.28301 2503.47543 ± 165.920
A 9941.18859 ± 257.929 6852.19607 ± 425.520
R-Square (COD 0.60285
Adj. R-Square 0.60223
Hg-183
B
A

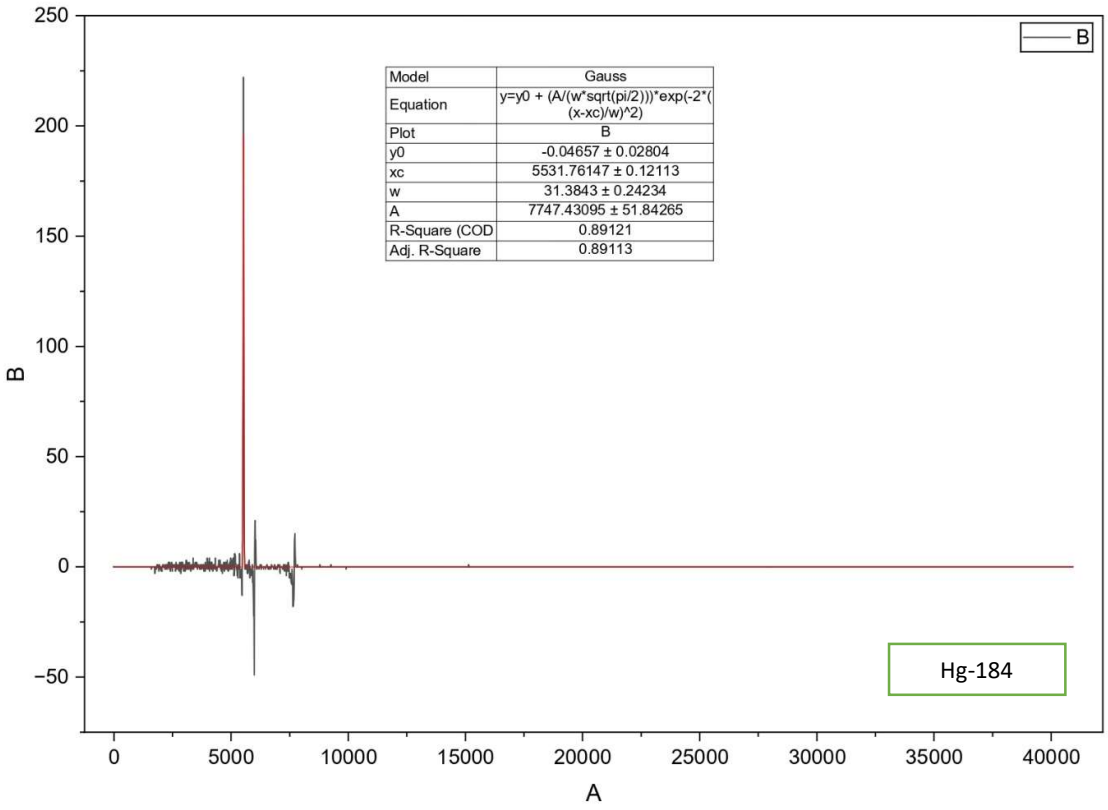
B
Model Gauss
Equation y=y0 + (A/(w*sqrt(pi/2)))*exp(-2*((x-xc)/w)^2)
Plot B
y0 -0.04657 ± 0.02804
xc 5531.76147 ± 0.12113
w 31.3843 ± 0.24234
A 7747.43095 ± 51.84265
R-Square (COD 0.89121
Adj. R-Square 0.89113
Hg-184
B
A

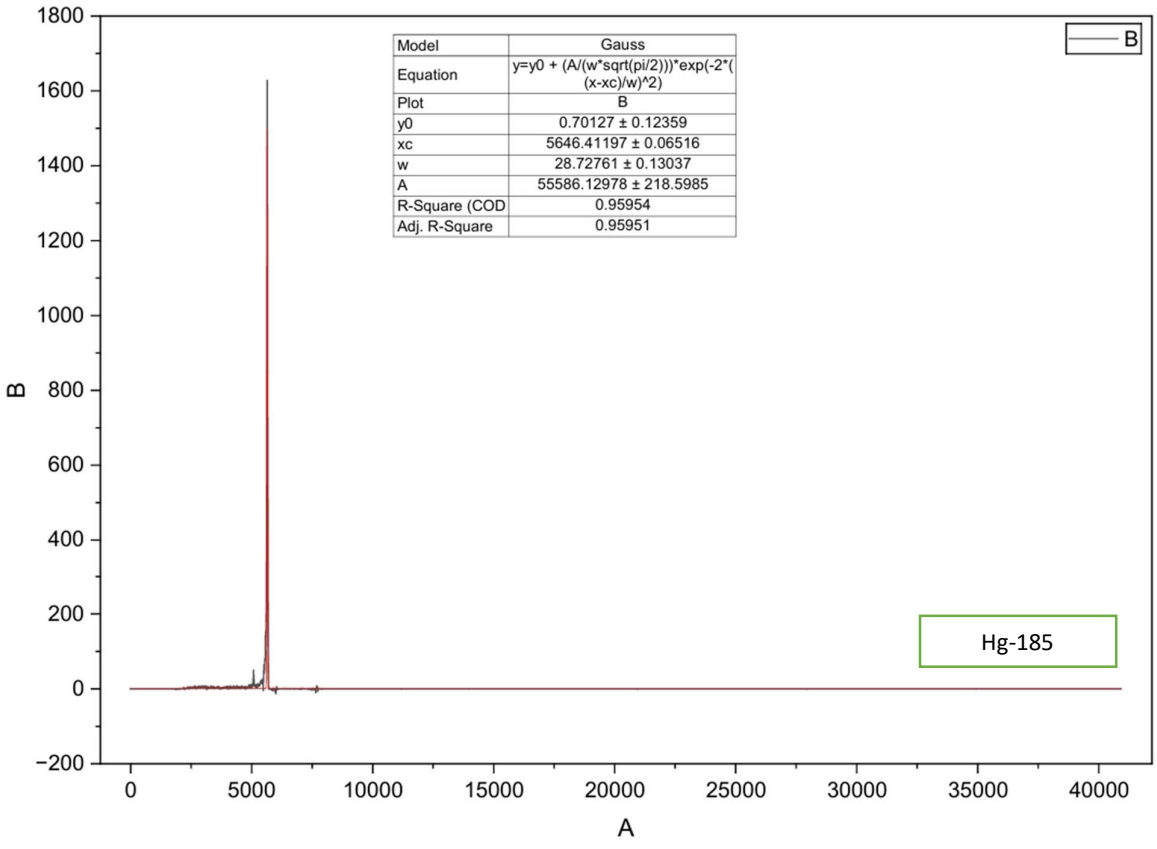
B
Model Gauss
Equation y=y0 + (A/(w*sqrt(pi/2)))*exp(-2*((x-xc)/w)^2)
Plot B
y0 0.70127 ± 0.12359
xc 5646.41197 ± 0.06516
w 28.72761 ± 0.13037
A 55586.12978 ± 218.5985
R-Square (COD 0.95954
Adj. R-Square 0.95951
Hg-185
B
A

Hg-180			
Detected peak (KeV)	Isotopes	Decay Energy (Kev)	Branching Ratio (%)
6111	Hg-180	6119	47.9
5752	Pt-176	5753	40

5. Energy-position matrix heat map for $^{40}Ar + ^{148}Sm$ reaction.

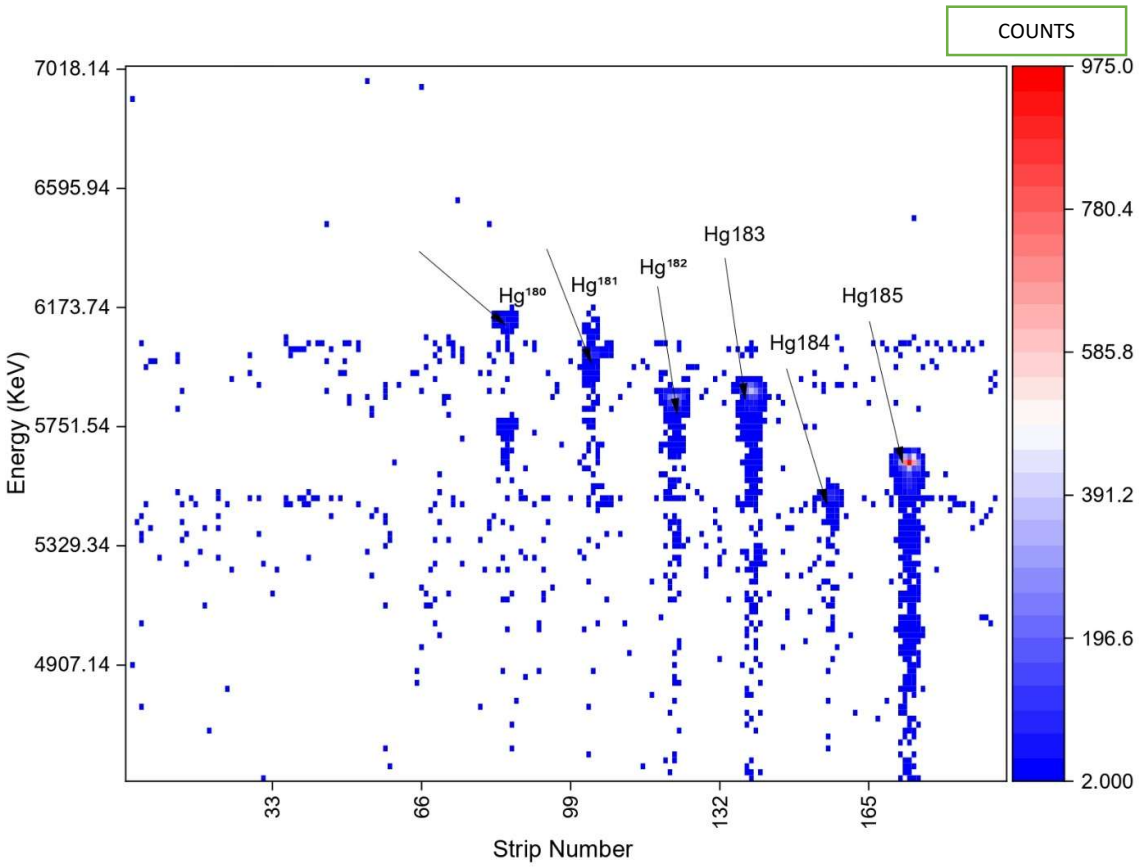

6. Histograms for Rn.($^{40}Ar + ^{166}Er$)

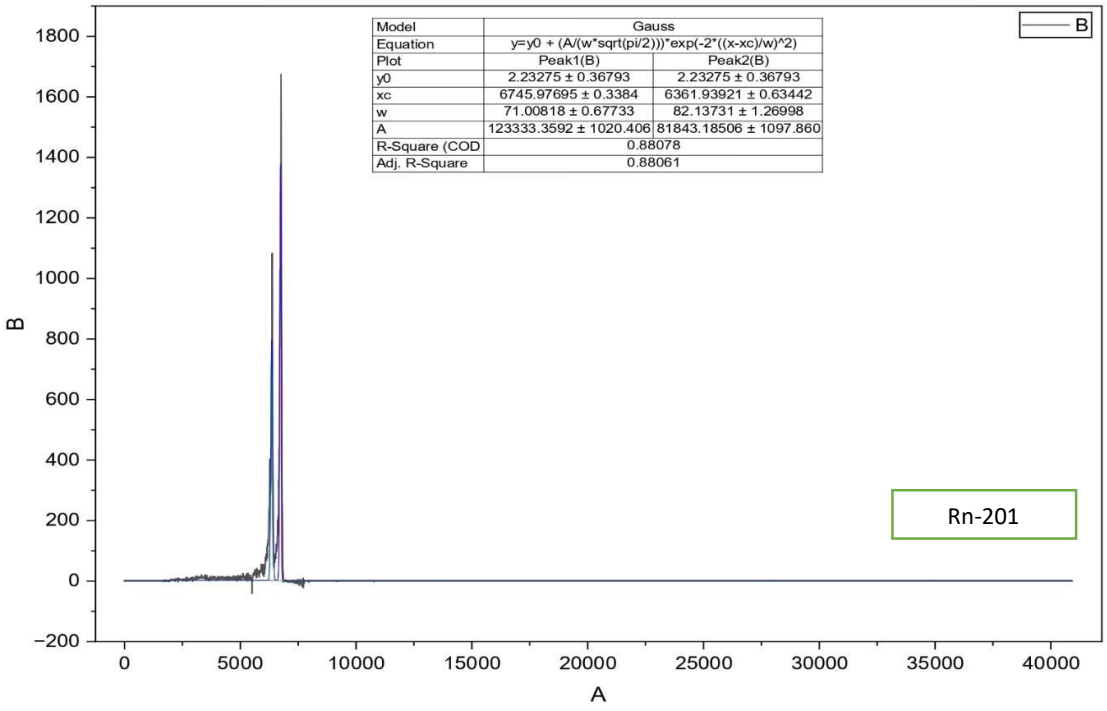

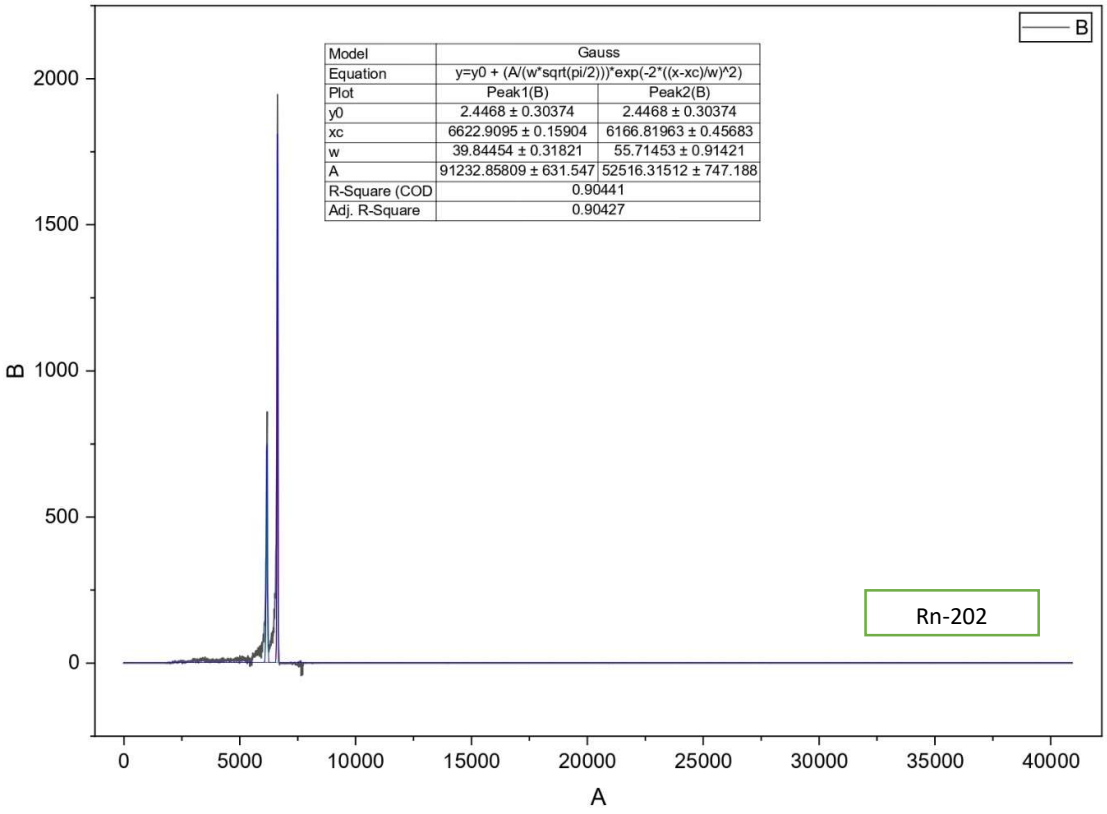

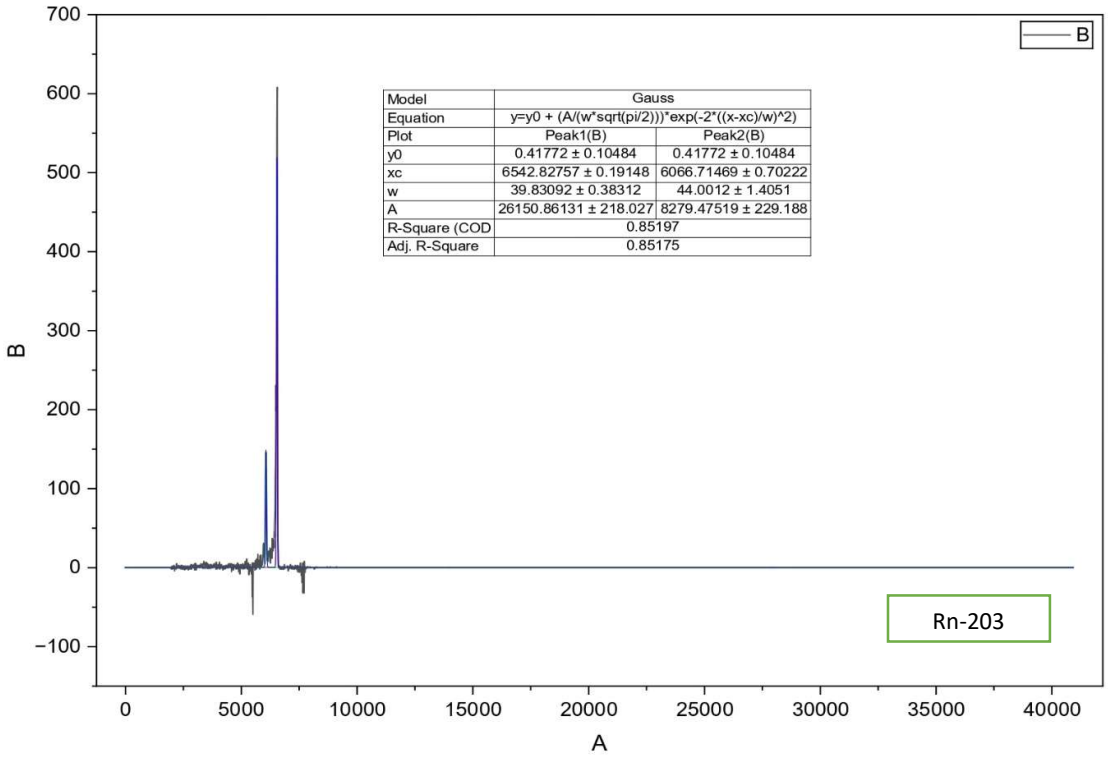
B
Model | Gauss
Equation | y=y0 + (A/(w*sqrt(pi/2)))*exp(-2*((x-xc)/w)^2)
Plot | Peak1(B) | Peak2(B)
y0 | 0.41772 ± 0.10484 | 0.41772 ± 0.10484
xc | 6542.82757 ± 0.19148 | 6066.71469 ± 0.70222
w | 39.83092 ± 0.38312 | 44.0012 ± 1.4051
A | 26150.86131 ± 218.027 | 8279.47519 ± 229.188
R-Square (COD | 0.85197
Adj. R-Square | 0.85175
Rn-203
B
A

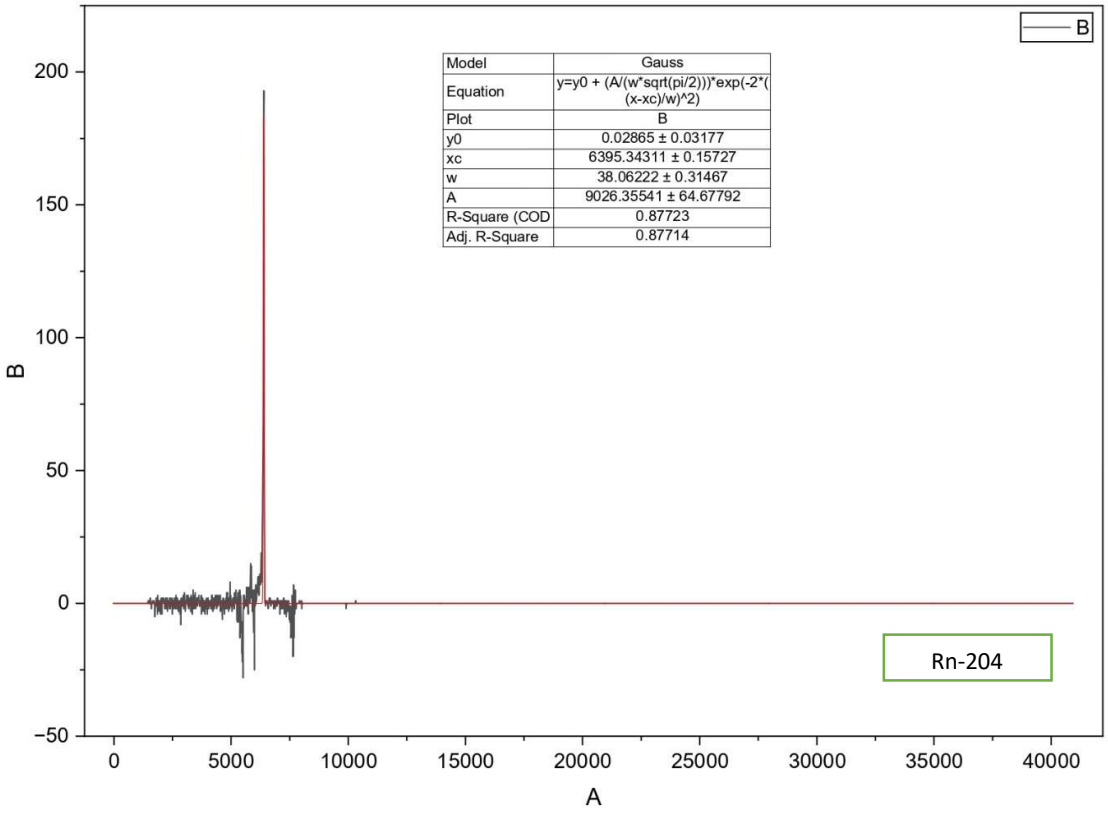
B
Model | Gauss
Equation | y=y0 + (A/(w*sqrt(pi/2)))*exp(-2*((x-xc)/w)^2)
Plot | B
y0 | 0.02865 ± 0.03177
xc | 6395.34311 ± 0.15727
w | 38.06222 ± 0.31467
A | 9026.35541 ± 64.67792
R-Square (COD | 0.87723
Adj. R-Square | 0.87714
Rn-204
B
A

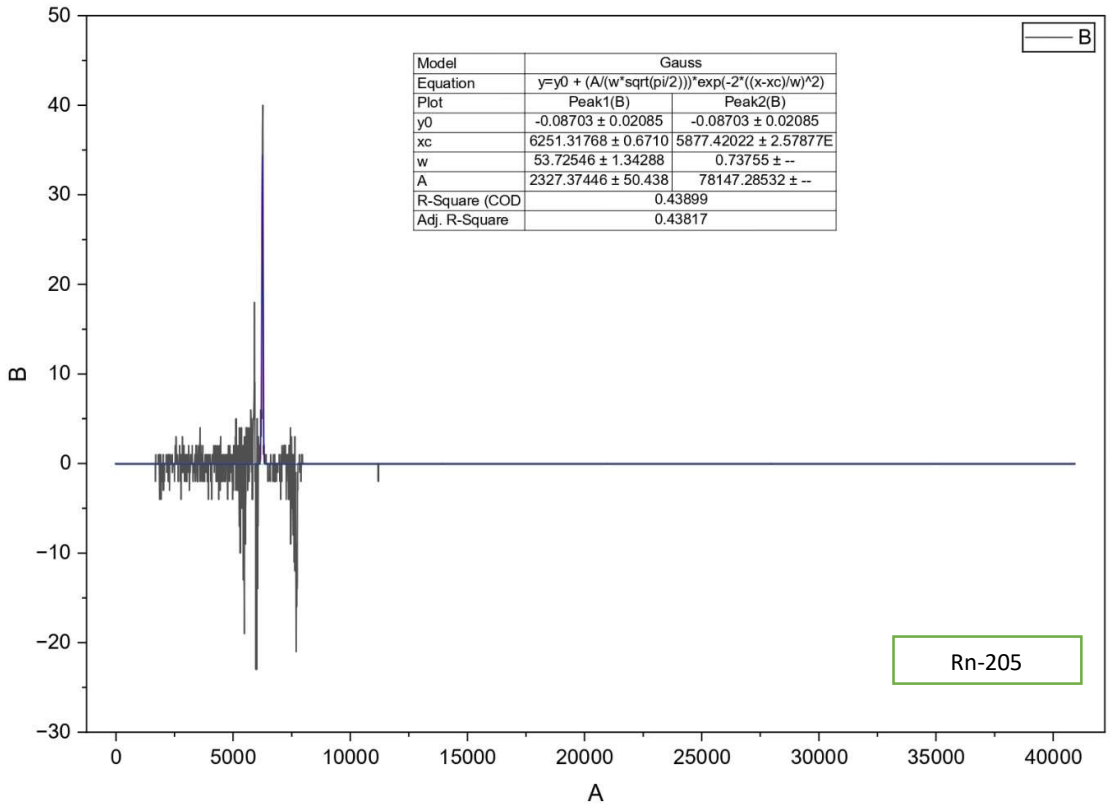
B
Model | Gauss
Equation | y=y0 + (A/(w*sqrt(pi/2)))*exp(-2*((x-xc)/w)^2)
Plot | Peak1(B) | Peak2(B)
y0 | -0.08703 ± 0.02085 | -0.08703 ± 0.02085
xc | 6251.31768 ± 0.6710 | 5877.42022 ± 2.57877E
w | 53.72546 ± 1.34288 | 0.73755 ± --
A | 2327.37446 ± 50.438 | 78147.28532 ± --
R-Square (COD | 0.43899
Adj. R-Square | 0.43817
Rn-205
B
A
50
40
30
20
10
0
−10
−20
−30
0
5000
10000
15000
20000
25000
30000
35000
40000

Rn-201			
Detected Peak (keV)	Isotopes	Decay Energy (KeV)	Branching Ratio (%)
6745	Rn-201	6773	90
6361	Po-197	6281	44

Rn-202			
Detected Peak (KeV)	Isotopes	Decay energy (KeV)	Branching Ratio (%)
6622	Rn-202	6639	78.8
6166	Po-198	6183	58

Rn-203			
Detected Peak (Kev)	Isotopes	Decay Energy (KeV)	Branching Ratio (%)
6066	Po-199	6059	39
6542	Rn-203	6550	75

7. Energy-position matrix heat map for $^{40}Ar + ^{166}Er$ reaction.

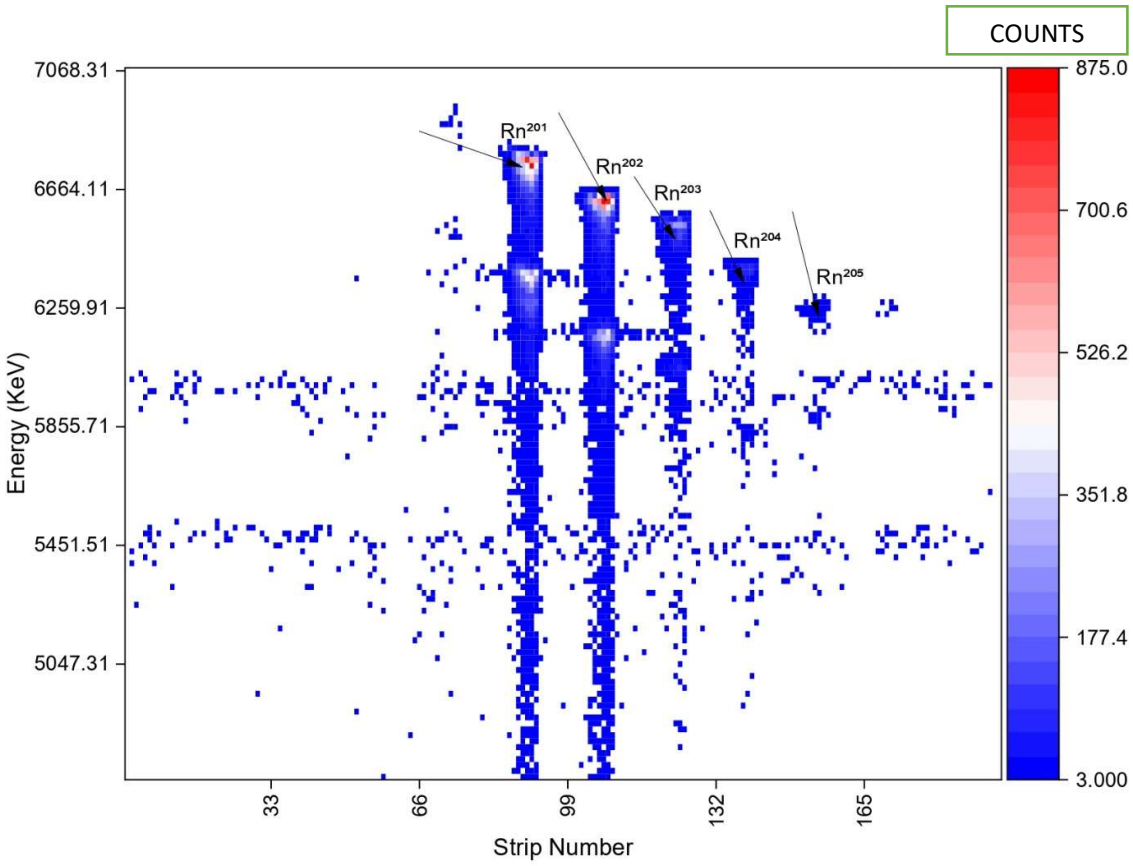

8. Histograms for Rn.($^{48}Ca + ^{242}Pu$)

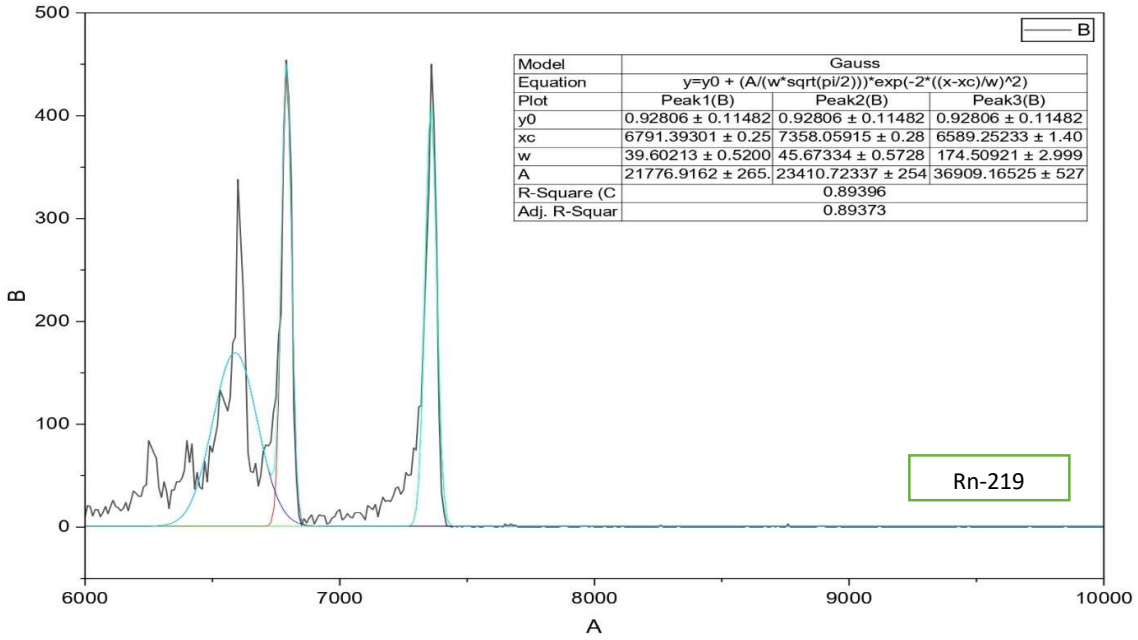

Model	Gauss					
Equation	y=y0 + (A/(w*sqrt(pi/2)))*exp(-2*((x-xc)/w)^2)					
Plot	Peak1(B)	Peak2(B)	Peak3(B)	Peak4(B)	Peak5(B)	Peak6(B)
y0	0.04972 ± 0.00546	0.04972 ± 0.00546	0.04972 ± 0.00546	0.04972 ± 0.00546	0.04972 ± 0.00546	0.04972 ± 0.00546
xc	4110.06867 ± 8.41927	5248.6927 ± 3.54851	7110.91623 ± 0.79063	7658.24649 ± 1.36765	6586.98885 ± 0.86998	7356.38074 ± 0.61262
w	165.59377 ± 16.86972	195.93175 ± 7.11257	25.72694 ± 1.58166	46.25429 ± 2.73672	50.75973 ± 1.74094	29.22347 ± 1.22564
A	259.01723 ± 22.93617	790.94831 ± 24.97402	168.9066 ± 8.99835	235.3907 ± 12.07389	425.41045 ± 12.65017	263.90215 ± 9.59156
R-Square (COD)	0.57712					
Adj. R-Square	0.57525					

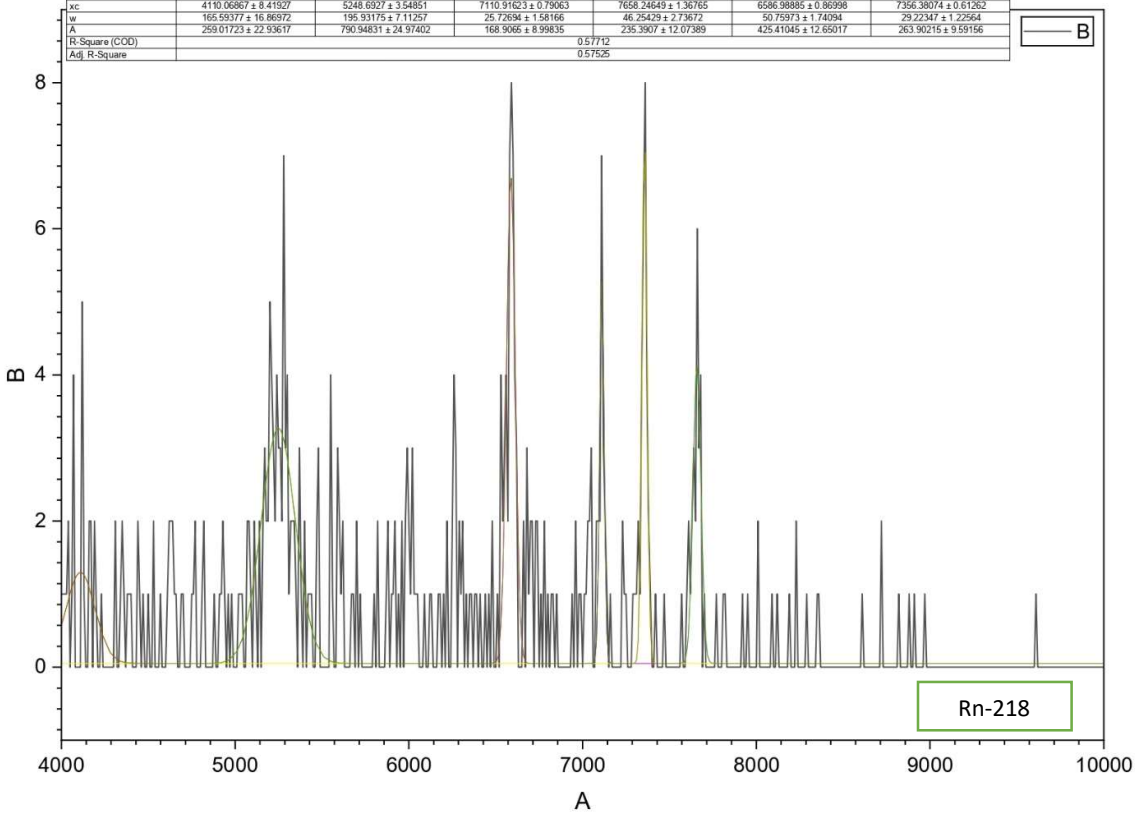

Data Set:[Rn212]Rn212!B Date:06-12-2025

BaseLine:Constant

Chi^2=2.21770E+00 Adj. R-Square=8.62920E-01 # of Data Points=3819

SS=8.46053E+03 Degrees of Freedom=3815

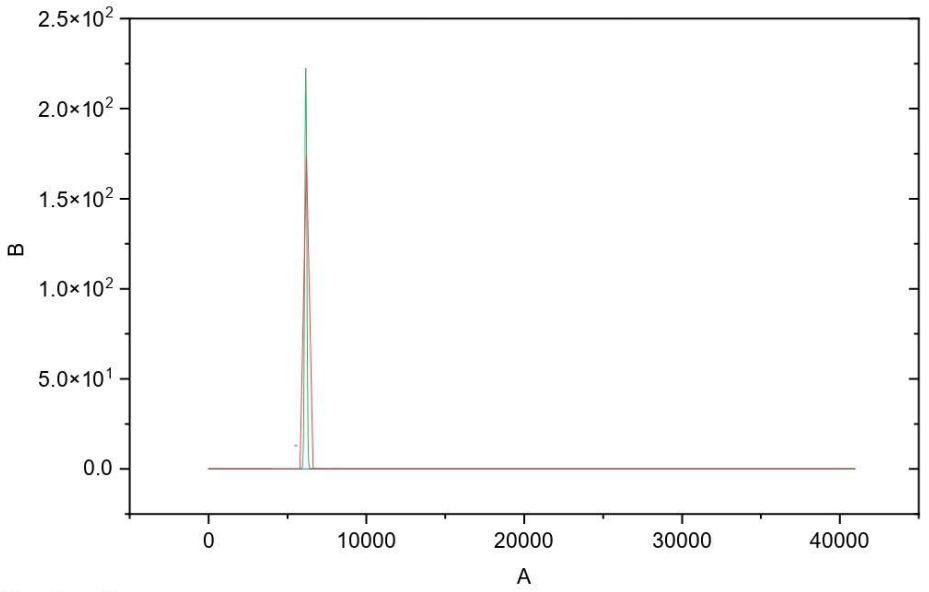

Fitting Results

Peak Index	Peak Type	Area Intg	FWHM	Max Height	Center Grvty	Area IntgP
1	Gaussian	71648.01655	154.86657	222.37623	6158.05718	100

Rn-212

Rn-219			
Detected Peak (KeV)	Isotopes	Decay Energy (KeV)	Branching Ratio
6791	Rn-219	6819	79.4
7358	Po-215	7386	99
6589	Rn-219	6552	12.9

9. Energy-position matrix heat map for $^{48}Ca + ^{242}Pu$ reaction

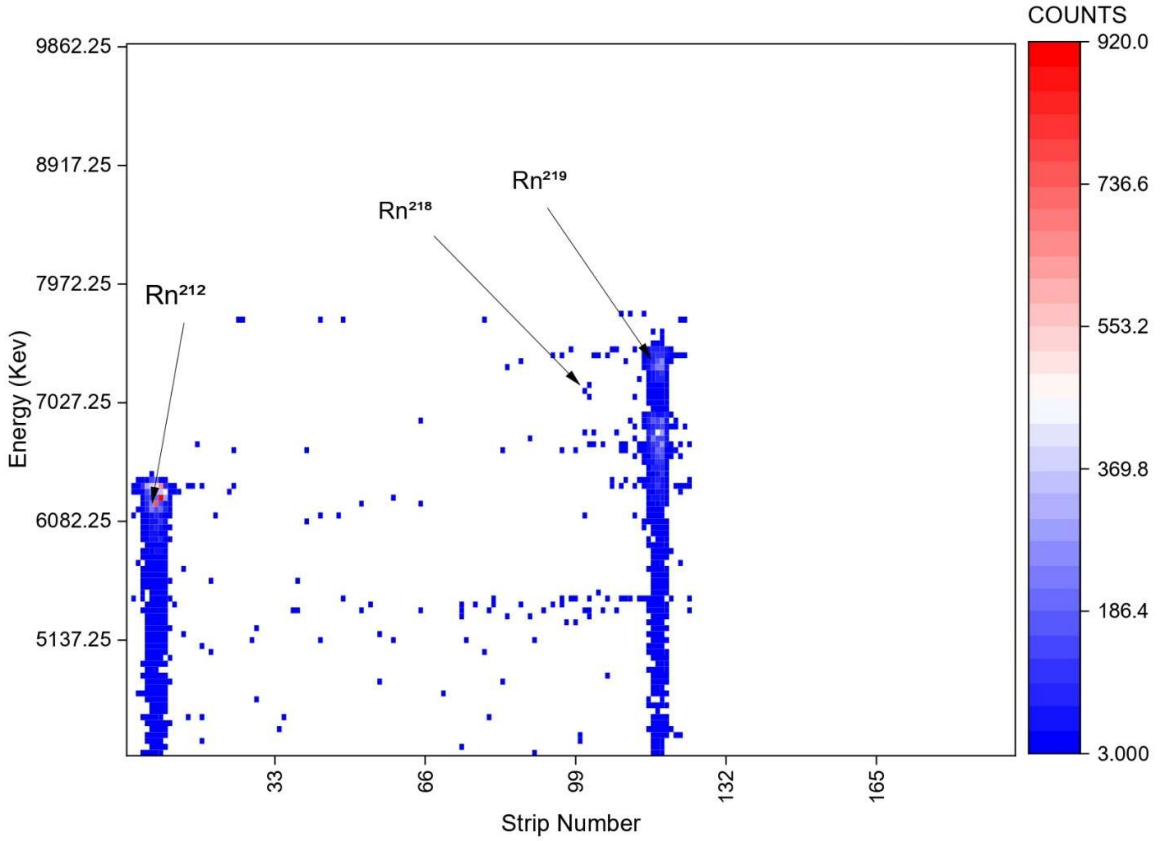

10.Conclusion

This study comprehensively validated the performance of the MASHA mass spectrometer in an analyzing products from heavy-ion fusion reactions relevant to the synthesis of superheavy elements. Using the ISOL method and an upgraded rotating target composed of carbon graphene nanotubes, significant improvements were achieved in ion separation efficiency, thermal stability, and measurement accuracy. The reactions $^{40}Ar + ^{148}Sm$ and $^{40}Ar + ^{166}Er$ effectively produced and identified mercury and radon isotopes, respectively, confirming the instrument's high mass resolution and detection precision. Minor challenges, such as beam purity affecting the identification of ^{205}Rn, highlight areas for further optimization.

using $^{48}Ca + ^{242}Pu$ demonstrated clear correlations between separation efficiency and isotope half-lives, particularly for ^{212}Rn and ^{219}Rn. The measured alpha energies exhibited excellent agreement with theoretical predictions, with deviations within 1–10 keV and FWHM values consistent with expected standards. Overall, the results reinforce the reliability of alpha spectrometry for isotope identification and nuclear decay mapping, supporting continued investigations into nuclear structure near the proton drip line. These advancements provide a robust foundation for future experiments aimed at discovering new superheavy nuclei within the predicted Island of Stability.

11.References

[1] Vedeneev, V. Y., Rodin, A. M., Krupa, L., Belozerov, A. V., Chernysheva, E. V., Dmitriev, S. N., Pospisil, S., et al.: The current status of the MASHA setup. Hyperfine Interactions 238, 1-14 (2017).

[2] Oganessian, Yu.Ts., Shchepunov, V.A., Dmitriev, S.N., et al.: The project of the mass separator of atomic nuclei produced in heavy ion induced reactions. Nucl. Inst. Methods B 204, 606–613 (2003).

[3] Rodin, A. M. Separation efficiency of the MASHA facility for short-lived mercury isotopes. Hyperfine Interact 227:209–221 (2014).

[4] Rodin, A. M.: MASHA Separator on the Heavy Ion Beam for Determining Masses and Nuclear Physical Properties of Isotopes of Heavy and Superheavy Elements. INSTRUMENTS AND EXPERIMENTAL TECHNIQUES 57(4): 386-393 (2014).

[5] Rodin, A. M., Chernysheva, E. V., Dmitriev, S. N., Gulyaev, A. V., Kamas, D., Kliman, J., ... & Yukhimchuk, S. A. (2020). Features of the solid-state isol method for fusion evaporation reactions induced by heavy ions. In Exotic Nuclei: Proceedings of the International Symposium on Exotic Nuclei (pp. 437-443).

[6] Efremov, A., Bekhterev, V., Bogomolov, S., Gulbekyan, G., Lebedev, A. N., Loginov, V. N., ... & Leporis, M. (2003). The 2.45 GHz ECR ion source for the first stage of the DRIBs project. Nuclear Instruments and Methods in Physics Research Section B: Beam Interactions with Materials and Atoms, vol.204, 368-371.

[7] Chernysheva, E. V., Rodin, A. M., Dmitriev, S. N., Gulyaev, A. V., Komarov, A. B., Novoselov, A. S., ... & Maher, A. (2020). Determination of Separation Efficiency of the Mass-Spectrometer MASHA by Means of Measurement of Absolute Cross Sections of Evaporation Residues. In Exotic Nuclei: Proceedings of the International Symposium on Exotic Nuclei (pp. 386-390).

[8] Веденеев, В. Ю., Родин, А. М., Крупа, Л., Камас, Д., Чернышева, Е. В., Гуляев, А. В., ... & Юхимчук, С. А. (2020). Сечения образования испарительных остатков реакций полного слияния 144 Sm (40 Ar, xn) 184–x Hg, 148 Sm (36 Ar, xn) 184–x Hg, 144 Nd (40 Ca, xn) 184–x Hg. Известия Российской академии наук. Серия физическая, 84(4), 594-598.